Digital Object Identifier 10.1109/PEDG54999.2022.9923312

2022 IEEE 13th International Symposium on Power Electronics for Distributed Generation Systems (PEDG)

A Passivity-Based High-Bandwidth Voltage Control for Grid-Forming Inverters

Alvaro Morales Munoz

Francisco D. Freijedo

Sante Pugliese

Marco Liserre

Suggested Citation

A. M. Munoz, F. D. Freijedo, S. Pugliese and M. Liserre, "A Passivity-Based High-Bandwidth Voltage Control for Grid-Forming Inverters," 2022 IEEE 13th International Symposium on Power Electronics for Distributed Generation Systems (PEDG), 2022, pp. 1-6, doi: 10.1109/PEDG54999.2022.9923312.

A Passivity-Based High-Bandwidth Voltage Control for Grid-Forming Inverters

Alvaro Morales Munoz, Francisco D. Freijedo
Huawei Nuremberg Research Center
Huawei Technologies Duesseldorf GmbH
Nuremberg, Germany
alvaro.morales.munoz@huawei.com, francisco.freijedo@huawei.com

Sante Pugliese, Marco Liserre
Chair of Power Electronics
Kiel University
Kiel, Germany
sapu@tf.uni-kiel.de, ml@tf.uni-kiel.de

***Abstract*—The increasing number of power electronic devices connected to the power system is leading it to new stability challenges. The uncertainty of the grid-model may complicate the controller design and compromise stability. As a counter-measure, LQR and pole-placement techniques can be re-oriented to design for passivity, which is leading to new controller design paradigms. Nevertheless, as a general rule, all the variables of the system are considered in the full bandwidth, which may become unfeasible or costly in the industrial scenario. An original controller design technique for LC or LCL filter which accomplishes passivity in a wide range of frequency is proposed. Besides, it reduces the voltage sensor needs, even controlling it, being suitable for Grid-Forming. As consequence, the complexity of the software, hardware and price are reduced. Experimental verification is provided: impedance of the converter from the grid side and response against a changes in the reference/load.**

***Index Terms*—Grid-connected converter, impedance shaping, LC/LCL filter, passivity, sensoring needs reduction.**

I. Introduction

Grid connected inverters are playing a main role in the power grid due to the increasing integration of power electronic interface renewable energy sources. As a consequence, the grid codes of the different countries are being updated in order to face this transformation [1]. One requirement that appears repeatably of main concerning is the system stability. Controller design plays a fundamental role in it. In fact, a controller can re-shape the output impedance of a power electronics converter in a specific frequency range, influencing its stability. Hence, passivity is a key concept to fulfill the stability requirements since it can ensure that energy is always dissipated in such device [2] [3].

Other important issues of grid connected inverters are synchronization process and power sharing with the grid. Grid-Forming (GFM) converters implementations based on power synchronization (e.g. synchronverter) aim to solve those issues. In their general structure an outer power control provides the voltage references for an inner voltage loop [4]. The proposed control, which can be classified as inner loop, is oriented to GFM since the controlled variable is the voltage.

Nowadays, manufacturers prefer to place a LC/LCL filter in the output of their inverters (Fig. 1) instead of a L filter because they can better remove the high frequency content due to the switching with a cheaper and more compact device. In return, an internal resonance is created, which should be damped.

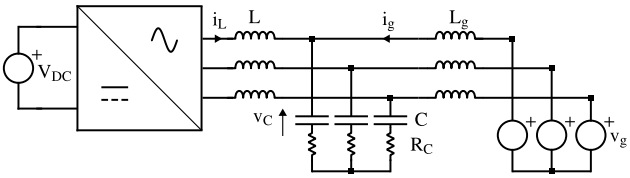

Fig. 1. Grid connected inverter by an LCL filter.

It can be done passively [5] which implies losses, so it is not the best solution, or via controller, avoiding them. Cascade control is one of the most used control technique [6]. However, the bandwidth is very low because control loops must be far away in the frequency range in order to avoid coupling between them. Hence, resonance is not always well damped. Thus, other techniques for damping can be applied [7]–[12]. One of the most common ways to achieve it is using State-Space (SSe) representation.

SSe control offers a wide variety of design methods, which can be applied to achieve AD. Poles placement using Ackermann technique is widely used. It allows to design the position of all the poles [7]. Designer must choose where poles should be placed (letting appear different criteria). The main disadvantages are: the solution is not always allowed and all the states of the system must be used [8]. Other design criterion [9] is to use Radial Projection. The poles are set very close to open-loop case. The main disadvantage is the non optimal solution given. Dead-Beat Control uses a different point of view, but it also applies Ackermann method [10]. The idea is to make the control as fast as possible, so a very high bandwidth is needed and passivity is also compromised. Other control design techniques are based on optimization: Linear Quadratic Regulator (LQR) or Discrete LQR (DLQR) [7] and Kalman Filter [11]. These methods reduce the problem to an optimization one. Hence, solutions are not always guarantee. The main difference between them is the chosen norm to be minimized. The physical meaning of the process is not always easy to follow and including passivity criterion fulfillment in the cost function does not seem straightforward.

In this paper a passivity-based pole placement using SSe representation is proposed. Passivity is achieved placing the poles in the fastest region without oscillating behaviour. For

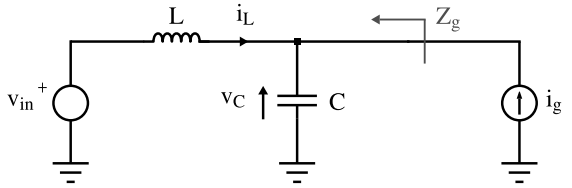

Fig. 2. Inverter and LC filter model.

that, only current state is requested without an estimator, which would be the method chosen by the previous investigations [7], [8] in order to obtain a sensor need reduction. Hence, there is no aliasing, less external disturbances and noise and no needs for oversampling. Voltage sensor is chosen to be simplified due to the fact that current signal is more filtered than voltage one i.e. better for measuring at high bandwidth. Therefore, cost, software and hardware complexity are reduced.

This work employs integral actions (resonant filter) for tracking, supported by a feed-forward term. The advantages are perfect tracking in a selected frequency, the base passive behaviour is affected in a narrow range and several of them with different frequencies can be set in parallel.

This paper starts describing the system, section II. Then, considerations for control design and the proposed control method appear, section III. Finally, the tests done in order to verify the controller are shown, section IV.

II. System Description

The model considered for voltage control is shown in Fig. 2, where the resistances are neglected ($R_C = 0$) in order to obtain the worst case from stability point of view. After that, applying a GFM technique, the system can be connected to the grid as Fig. 1.

$$\begin{aligned} \frac{di_L(t)}{dt} &= -\frac{v_C(t)}{L} + \frac{v_{in}(t)}{L} \\ \frac{dv_C(t)}{dt} &= \frac{i_L(t)}{C} + \frac{i_g(t)}{C} \end{aligned} \tag{1}$$

Those can be merged using SSe representation, (2).

The controller is digital. Hence, a discrete domain representation (3) is more accurate with reality. The PWM can be modeled as Zero-Order Hold (ZOH), then, the discretization is (4). It includes half cycle delay ($0.5T_s$).

$$\begin{aligned} x(k+1) &= \phi x(k) + \Gamma u(k) \\ y(k) &= \Psi x(k) \end{aligned} \tag{3}$$

Ψ is a matrix will be composed by unitary or zero vectors depending on the variable of interest.

$$\begin{aligned} \phi &= e^{AT_s} \\ \Gamma &= \int_0^{T_s} e^{A\tau} d\tau B = (e^{AT_s} - I)A^{-1}B \end{aligned} \tag{4}$$

The result is given by (5). Previously, for sake of clarity, several substitutions are done.

$$\begin{aligned} a &= \cos(\frac{T_s}{\sqrt{LC}}) \\ b &= \sqrt{\frac{C}{L}}\sin(\frac{T_s}{\sqrt{LC}}) \\ c &= \sqrt{\frac{L}{C}}\sin(\frac{T_s}{\sqrt{LC}}) \end{aligned} \tag{6}$$

However, the delay due to the data acquisition, one cycle, is missing [11]. To that end, the actuated variable will receive the information one cycle later [7].

$$\begin{aligned} v_d(k+1) &= v_{in}(k) \\ x(k+1) &= \underbrace{\begin{bmatrix} \phi & \Gamma_1 \\ 0 & 0 \end{bmatrix}}_{\Phi'} x(k) + \underbrace{\begin{bmatrix} 0 \\ 1 \end{bmatrix}}_{\Gamma_1'} u_1(k) + \underbrace{\begin{bmatrix} \Gamma_2 \\ 0 \end{bmatrix}}_{\Gamma_2'} u_2(k) \\ y(k) &= \Psi x(k) \end{aligned} \tag{7}$$

Finally, moving the discrete domain to the Z-domain, the final system is (8).

III. Proposed Controller

A. Passivity Controller Design

First, the most internal layer is explained. The main goal is to keep passivity. That means the angle of the frequency response must be between $+90^o$ and -90^o. For that, a control law which involves proportional gains is applied.

$$v_{in}(z) = -Kx(z) = -\begin{bmatrix} K_I & K_v & K_d \end{bmatrix} x(z) \tag{9}$$

The next step is obtaining the transfer functions matrix, which will have the same poles for all the states.

$$\begin{aligned} x(z) &= (zI - \phi' + \Gamma_1' K)^{-1}\Gamma_2' u(z) \\ y(z) &= \Psi' x(z) \end{aligned} \tag{10}$$

$$\text{Characteristic Equation} \equiv |zI - \phi' + \Gamma_1' K| \tag{11}$$

Ψ' allows to choose the desired transfer function. The poles set is given by the characteristic equation. Hence, introducing the model (8) in (11) gives the poles of the full system.

$$\begin{aligned} z^3 + (K_d - 2a)z^2 + (K_V + 1 - 2K_d a - K_V a + K_I b)z \\ + (-K_I b - K_V a + K_d + K_V) = 0 \end{aligned} \tag{12}$$

Forcing K_I or K_V to be 0 means this value is not measured i.e. the sensor is removed for stability purpose. Comparing measurements, current and voltage have differences. The first one is preferred due to the inductive behaviour of the electrical circuits. It acts like a low pass filter, cleaving a more clean signal for measuring. Thus, the choice is $K_V = 0$.

Applying this modification into (12), the equation offers 3 poles, which can be separated into a pair of poles and a single pole, and only 2 variables to modify.

$$\frac{d}{dt}\begin{bmatrix} i_L(t) \\ v_C(t) \end{bmatrix} = \underbrace{\begin{bmatrix} 0 & -\frac{1}{L} \\ \frac{1}{C} & 0 \end{bmatrix}}_{A} \begin{bmatrix} i_L(t) \\ v_C(t) \end{bmatrix} + \underbrace{\begin{bmatrix} \frac{1}{L} \\ 0 \end{bmatrix}}_{B_1} v_{in}(t) + \underbrace{\begin{bmatrix} 0 \\ \frac{1}{C} \end{bmatrix}}_{B_2} i_g(t) \tag{2}$$

$$\begin{bmatrix} i_L(k+1) \\ v_C(k+1) \end{bmatrix} = \underbrace{\begin{bmatrix} a & -b \\ c & a \end{bmatrix}}_{\Phi} \begin{bmatrix} i_L(k) \\ v_C(k) \end{bmatrix} + \underbrace{\begin{bmatrix} b \\ 1-a \end{bmatrix}}_{\Gamma_1} v_{in}(k) + \underbrace{\begin{bmatrix} -1+a \\ c \end{bmatrix}}_{\Gamma_2} i_g(k) \tag{5}$$

$$z\begin{bmatrix} i_L(z) \\ v_C(z) \\ v_d(z) \end{bmatrix} = \underbrace{\begin{bmatrix} a & -b & b \\ c & a & 1-a \\ 0 & 0 & 0 \end{bmatrix}}_{\Phi'} \begin{bmatrix} i_L(z) \\ v_C(z) \\ v_d(z) \end{bmatrix} + \underbrace{\begin{bmatrix} 0 \\ 0 \\ 1 \end{bmatrix}}_{\Gamma_1'} v_{in}(z) + \underbrace{\begin{bmatrix} -1+a \\ c \\ 0 \end{bmatrix}}_{\Gamma_2'} i_g(z) \tag{8}$$

$$z^3 + (K_d - 2a)z^2 + (1 - 2K_d a + K_I b)z + (-K_I b + K_d) = 0 \tag{13}$$

The solution is obtained by comparison.

$$\begin{aligned} (z^2 + hz + n)(z + m) &= 0 \\ z^3 + (h+m)z^2 + (hm+n)z + mn &= 0 \end{aligned} \tag{14}$$

$$\begin{aligned} h + m &= K_d - 2a \\ hm + n &= 1 - 2K_d a + K_I b \\ nm &= -K_I b + K_d \end{aligned} \tag{15}$$

As it was said before, there are two freedom degrees. One of them is used to set the single pole, imposing the frequency of m.

$$z = -m = -e^{-T_s \omega} \tag{16}$$

The other is used to set a critically damped pair of poles (stability is key):

$$\begin{aligned} z &= \frac{-h}{2} \pm \sqrt{\frac{h^2 - 4n}{4}} \\ h^2 &= 4n \end{aligned} \tag{17}$$

At this point, all parameters can be defined by fixing the frequency of the single pole i.e. the value of m. In the high-frequency range the control loses influence and the system tends to behave as open-loop [3]. The poles should therefore be pushed to this area where the delaying effect of the controller (see phase decay in Fig. 5) becomes less relevant.

As the single pole is pushed to higher frequency, the pair of poles become slower and vice-versa. For this reason, the optimal distribution occurs when all the poles are located at the same frequency, m_{ot}. The equivalent expression in (14) can then be substituted by:

$$\begin{aligned} (z + m_{ot})^3 &= 0 \\ z^3 + 3m_{ot}z^2 + 3m_{ot}^2 z + m_{ot}^3 &= 0 \end{aligned} \tag{18}$$

Where comparing to (13) as done in (15) and rearranging, the expressions for gains and optimum frequency m_{ot} are obtained:

$$\begin{aligned} m_{ot}^3 + 3m_{ot}^2 + (-3 + 6a)m_{ot} + (-1 + 4a^2 - 2a) &= 0 \\ K_d &= 3m_{ot} + 2a \\ K_I &= \frac{-m_{ot}^3 + 3m_{ot} + 2a}{b} \end{aligned} \tag{19}$$

The impedance transfer function, where passivity can be checked, Fig. 2, is,

$$Z_g(z) = \frac{-cz^2 + c\,(1 - K_d)\,z + (cK_d + 2\,(a-1)\,K_I)}{z^3 + (K_d - 2a)z^2 + (1 - 2K_d a + K_I b)z + (-K_I b + K_d)} \tag{20}$$

Note: At high frequency the system start to behave in open-loop, but the delay effect which try to send the system to a non-passive region is still present. Therefore, passivity could be broken. This can be solved adding a small resistance in the capacitor leg, following [13].

B. Tracking Controller Design

With the previous development, base behaviour of the inverter is set. The next point to cover is to follow a/several reference/s for the capacitor voltage.

1) Resonant controller tuning and modeling: A controller which only affects the system in the reference frequency is needed. Therefore, one the best options is resonant filter. Moreover, it allows to use a voltage sensor with a low bandwidth (usually, only fundamental and low-order harmonics are targeted for high-gain control).

$$G_r(z) = K_r \frac{\cos(\omega_0 T_s)s - \omega_0 \sin(\omega_0 T_s)}{s^2 + \omega_0^2} \tag{21}$$

Where ω_0 is the resonant frequency and gains in the numerator are set to compensate the effect of the delay [14], allowing to be inside of the passivity range. K_r sets the sensitiveness and convergence speed. There are several ways

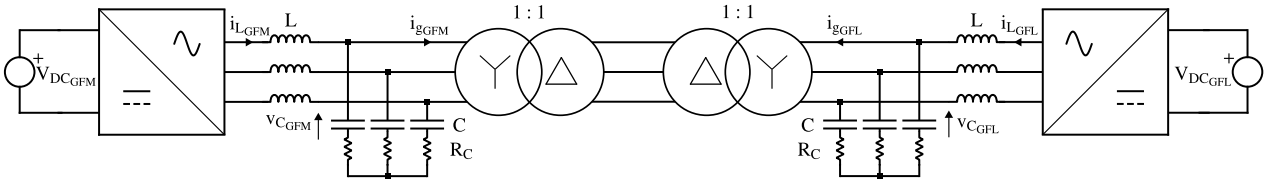

Fig. 3. Experimental Setup representation.

$$v_C(z) = \frac{(1-a)(z+1)}{(z+m)^3} v_{in}(z) + \frac{-cz^2 + c(1-K_d)z + (cK_d + 2(a-1)K_I)}{(z+m)^3} i_g(z) \tag{24}$$

to achieve them in discrete domain [15]. Zero-Pole Matching technique is chosen because it is strictly proper:

$$G_{rd}(z) = \frac{K_2 z^{-1} + K_1 z^{-2}}{1 - 2\cos(\omega_0 T_s) z^{-1} + z^{-2}} \tag{22}$$

K_1 and K_2 are, from discretization:

$$\begin{aligned} K_1 &= \frac{K_r \sin(\omega_0 T_s)(2 - 2\cos(\omega_0 T_s))}{\omega_0 \left(1 - e^{-\omega_0 \tan(\omega_O T_s) T_s}\right)} e^{\omega_0 \tan(\omega_0 T_s) T_s} \\ K_2 &= K_r \frac{\sin(\omega_0 T_s)(2\cos(\omega_0 T_s) - 2)}{\omega_0 \left(1 - e^{\omega_0 \tan(\omega_0 T_s) T_s}\right)} \end{aligned} \tag{23}$$

K_r tuning is obtained by experimental adjustment. Several bode graphs can be plotted with different K_r values: bigger value, faster response but higher bandwidth affected. If there are several resonant filters in parallel, their effect cannot be overlapped. Hence, K_r value depends on the application. As capacitor voltage is the tracked parameter, the bode plot to consider is $\frac{v_C(z)}{i_o(z)}$.

The resonant controller can be added to the SSe representation like in [7], [11]. Then, with the next system, the transfer function for tuning the resonant controller can be obtained applying (10).

2) Feed-forward Term: The controlled variable, v_C, is affected by two inputs: the input voltage v_{in} and the grid current i_g, which is the disturbance, as is shown in (8). Including passivity controller, v_C behaviour is represented by (24).

A faster and more robust response can be obtained adding a feed-forward term to the control law: the reference signal v_{ref} and its gain. This gain is calculated assuming that there are no resonant controller, no perturbation and the reference signal frequency (usually $50/60\,Hz$) is close to $0\,Hz$. Therefore, the new input is $v_{in} = -K_I i_L - K_d v_d + K_{ref} v_{ref}$. And K_{ref} is obtained using the first part of (24):

$$\left.\frac{v_C(z=1)}{v_{ref}(z=1)}\right|_{i_g=0} = 1 \tag{25}$$

The solution is:

$$K_{ref} = K_d + 1 \tag{26}$$

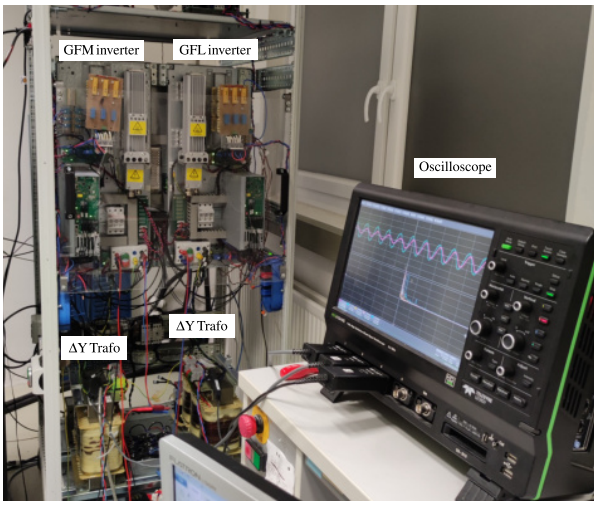

Fig. 4. Experimental Setup.

3) Anti-Windup: Tracking task relies on resonant controller and feed-forward term. If the first one does not exists, the second one will follow the reference signal but there will be always an error due to the disturbance effect, i_g. This fact can be useful for defining an anti-windup: The resonant controller could skyrocket if the system touch its saturation limit. In this moment, the resonant controller is reset. When the requested voltage is lower than the saturation level, the resonant part can be reconnected.

IV. Experimental Verification

Experiments were carried on using 2 inverters Danfoss FC-302, $4kVA$ each, with their filters, as it is shown in Fig. 3 and 4. The values of the parameters are collected in the table I. One inverter works as a voltage source i.e. as a GFM inverter. The other inverter works as a current source i.e. as a Grid Following (GFL) inverter.

The control method proposed for GFM inverter was uploaded in a dSpace control desk, applying the values from table I. Synchronous sampling, with double update is used. GFL control was also upload in a similar board, without double update. The inverters were not synchronized between them.

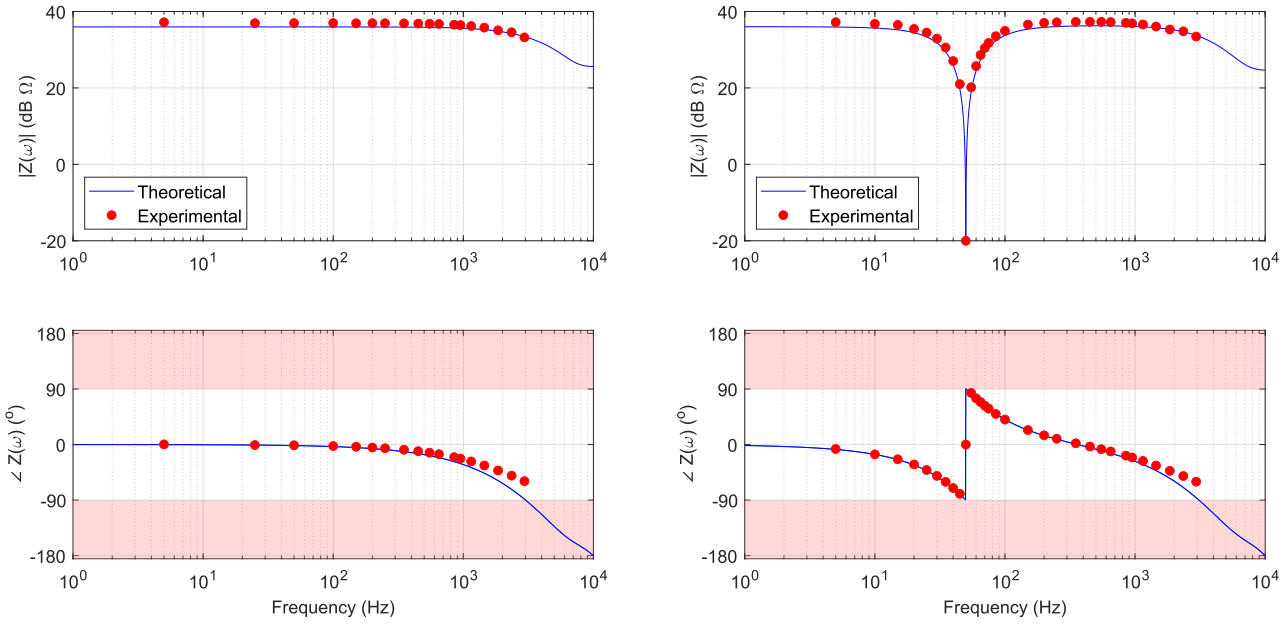

(a) Without Resonant Controller

(b) With Resonant Controller

Fig. 5. Frequency Impedance Response.

TABLE I
PARAMETERS AND CONTROLLER GAINS VALUES

Parameter	Value	Gain	Value
L	$5.03\,mH$	K_I	148.5530
C	$1.5\,\mu F$	K_d	1.4102
R_C	$2\,\Omega$	K_1'	-0.05000
$f_{sp_{GFM}}$	$20\,kHz$	K_2'	0.04999
f_{swGFM}	$10\,kHz$	K_{ref}	2.4102
$f_{sp_{GFL}}$	$10\,kHz$		
f_{swGFL}	$10\,kHz$		
$V_{DC_{GFM}}$	$790\,V$		
$V_{DC_{GFL}}$	$790\,V$		

A. Impedance Response

GFL inverter injects $i_{g_{GFL}}$ in a fix frequency. Hence, $i_{g_{GFM}}$ will have the same frequency. GFM inverter response at this frequency is read: $v_{C_{GFM}}$. Repeating the process for different frequencies (frequency sweep), the impedance response is obtained, (27). The injected current is controlled by a resonant controller in GFL inverter. $v_{C_{GFM}}$ and $i_{g_{GFM}}$ measurements are done by Phase-Locked Loop, one for each.

$$\begin{aligned} |Z(j\omega)| &= \frac{|v_C(j\omega)|}{|i_g(j\omega)|} \\ \angle Z(j\omega) &= \angle v_C(j\omega) - \angle i_g(j\omega) \end{aligned} \tag{27}$$

However, the controlled variable, v_C depends also on v_{in}, hence, on v_{ref}. This is easily understood looking at (24). In order to avoid the influence of this parameter, the reference signal must be 0.

The results are presented in Figs. 5. The first one shows the response without the tracking control method and the second one, with it. Also, the expected response is plotted. It is obtained with the model (10). In this case, the capacitor leg resistance cannot be neglected. Due to this reason, an error appears between the theoretical and the experimental results.

Passivity is fulfilled in the tested range. At higher frequency, the system tends to operate in open-loop, so the passivity maintenance is expected. This is reflected in the divergence between experiments results and model at high frequency.

B. Response against variations

This test shows the performance for tracking a reference signal at $50\,Hz$. The configuration is kept as in Fig. 3. First of all, a reference step from $200\,V$ to $300\,V$ is done, while the current is kept at $5\,A$, Fig. 6. In the current, a strong distortion can be appreciated. This is due to the non-linear effects of the transformers. Also, its amplitude, which should be constant (GFL inverter is regulating it), changes because GFL controller does not completely reject its disturbance.

Secondly, a current change is done, going from $1\,A$ to $5\,A$, while the voltage is kept at $300\,V$, Fig. 7. This one cannot be considered as a step due to the slow response of the GFL inverter. It is closer to a ramp. Again, the current distortion due to the transformers appears.

V. CONCLUSION

This paper proposes a design method for direct capacitor voltage control of a LC filter plus inverter; the technique is

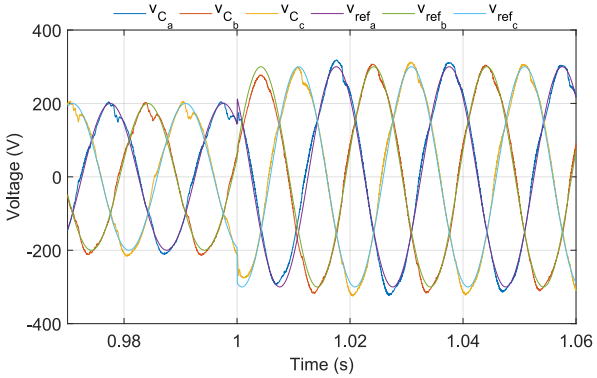

(a) Capacitor voltages and the references, GFM inverter

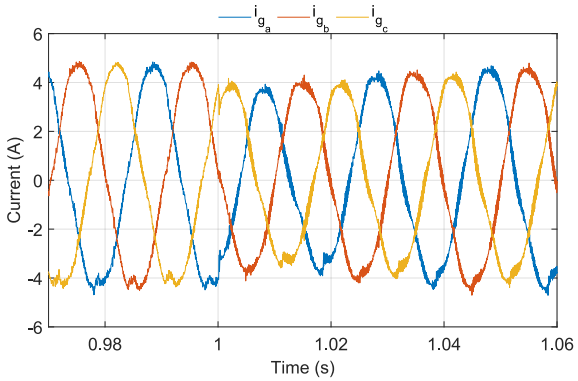

(b) Grid Currents, GFM inverter

Fig. 6. Reference Step from 200 V to 300 V at 1 s.

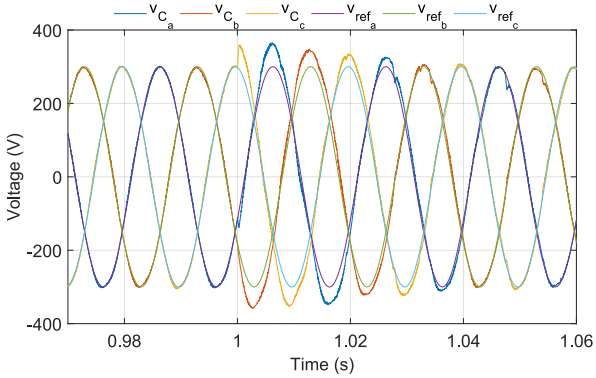

(a) Capacitor voltages and the references, GFM inverter

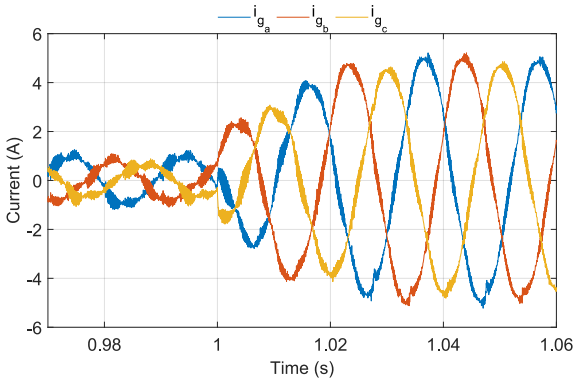

(b) Grid Currents, GFM inverter

Fig. 7. Grid current change from 1 A to 5 A at 1 s.

ready for plug-in a GFM technique that will be addressed in future works. The main task solved by it are: damping of the filter resonance, passivity in a very wide range of frequencies and decreasing the need of voltage sensor, saving costs. For tracking a reference signal, resonant controller is implemented. Experimental validation proves the performances of the proposed model.

References

[1] National Grid ESO, *GC0137: Minimum Specification Required for Provision of GB Grid Forming (GBGF) Capability*, 02 2022.

[2] J. Bao and L. Peter, *Process Control: The Passive Systems Approach*, 2007.

[3] F. D. Freijedo, M. Ferrer, and D. Dujic, "Multivariable high-frequency input-admittance of grid-connected converters: Modeling, validation, and implications on stability," *IEEE Trans. on Ind. Electr.*, vol. 66, no. 8, pp. 6505–6515, 2019.

[4] R. Rosso, X. Wang, M. Liserre, X. Lu, and S. Engelken, "Grid-forming converters: Control approaches, grid-synchronization, and future trends—a review," *IEEE Open Journal of Ind. App.*, vol. 2, pp. 93–109, 2021.

[5] R. Peña-Alzola, M. Liserre, F. Blaabjerg, R. Sebastián, J. Dannehl, and F. W. Fuchs, "Analysis of the passive damping losses in lcl-filter-based grid converters," *IEEE Trans. on Ind. Electr.*, vol. 28, no. 6, pp. 2642–2646, 2013.

[6] V. Pirsto, J. Kukkola, F. M. Mahafugur Rahman, and M. Hinkkanen, "Weak-grid tolerant positive- and negative-sequence current control of voltage-source converters," in *2021 IEEE PES Innovative Smart Grid Technologies Europe (ISGT Europe)*, 2021, pp. 01–06.

[7] G. Franklin, J. Powell, and M. Workman, *Digital Control of Dynamic Systems-Third Edition*, 1998.

[8] J. Kukkola, M. Hinkkanen, and K. Zenger, "Observer-based state-space current controller for a grid converter equipped with an lcl filter: Analytical method for direct discrete-time design," *IEEE Trans. on Ind. App.*, vol. 51, no. 5, pp. 4079–4090, 2015.

[9] D. Pérez-Estévez, J. Doval-Gandoy, A. G. Yepes, and s. López, "Positive- and negative-sequence current controller with direct discrete-time pole placement for grid-tied converters with lcl filter," *IEEE Trans. Power Electr.*, vol. 32, no. 9, pp. 7207–7221, 2017.

[10] S. Moon, J.-M. Choe, and J.-S. Lai, "Design of a state-space controller employing a deadbeat state observer for ups inverters," in *2017 Asian Conference on Energy, Power and Transportation Electrification (ACEPT)*, 2017, pp. 1–6.

[11] D. Pérez-Estévez, J. Doval-Gandoy, A. G. Yepes, s. López, and F. Baneira, "Generalized multifrequency current controller for grid-connected converters with lcl filter," *IEEE Trans. on Ind. App.*, vol. 54, no. 5, pp. 4537–4553, 2018.

[12] C. Lascu, "Sliding-mode direct-voltage control of voltage-source converters with lc filters for pulsed power loads," *IEEE Trans. on Ind. Electr.*, vol. 68, no. 12, pp. 11 642–11 650, 2021.

[13] E. Rodriguez-Diaz, F. D. Freijedo, J. M. Guerrero, J.-A. Marrero-Sosa, and D. Dujic, "Input-admittance passivity compliance for grid-connected converters with an lcl filter," *IEEE Trans. on Ind. Electr.*, vol. 66, no. 2, pp. 1089–1097, 2019.

[14] A. G. Yepes, F. D. Freijedo, s. Lopez, and J. Doval-Gandoy, "Analysis and design of resonant current controllers for voltage-source converters by means of nyquist diagrams and sensitivity function," *IEEE Trans. on Ind. Electr.*, vol. 58, no. 11, pp. 5231–5250, 2011.

[15] A. G. Yepes, F. D. Freijedo, J. Doval-Gandoy, s. López, J. Malvar, and P. Fernandez-Comesaña, "Effects of discretization methods on the performance of resonant controllers," *IEEE Trans. on Power Electr.*, vol. 25, no. 7, pp. 1692–1712, 2010.